Synthesis of Highly Fluorescent Metal (Ag, Au, Pt, and Cu) Nanoclusters by Electrostatically Induced Reversible Phase Transfer

Xun Yuan,[†] Zhentao Luo,[†] Qingbo Zhang,[†] Xinhai Zhang,[‡] Yuangang Zheng,[‡] Jim Yang Lee,[†] and Jianping Xie[†,*]

[†]Department of Chemical and Biomolecular Engineering, National University of Singapore, 10 Kent Ridge Crescent, Singapore 119260, and [‡]Institute of Materials Research and Engineering, 3 Research Link, Singapore 117602

ABSTRACT

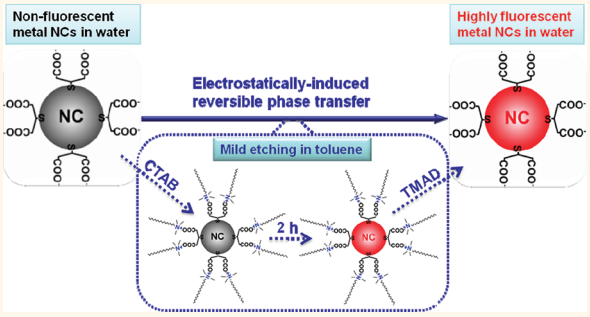

This paper reports a simple and scalable method for the synthesis of highly fluorescent Ag, Au, Pt, and Cu nanoclusters (NCs) based on a mild etching environment made possible by phase transfer *via* electrostatic interactions. Using Ag as a model metal, a simple and fast (total synthesis time < 3 h) phase transfer cycle (aqueous → organic (2 h incubation) → aqueous) has been developed to process originally polydisperse, nonfluorescent, and unstable Ag NCs into monodisperse, highly fluorescent, and extremely stable Ag NCs in the same phase (aqueous) and protected by the same thiol ligand. The synthetic protocol was successfully extended to fabricate highly fluorescent Ag NCs protected by custom-designed peptides with desired functionalities (*e.g.*, carboxyl, hydroxyl, and amine). The facile synthetic method developed in this study should largely contribute to the practical applications of this new class of fluorescence probes.

KEYWORDS: nanoclusters · metal nanomaterials · silver · phase transfer · fluorescence

Noble metal nanoclusters (NCs) are defined as isolated particles less than 2 nm in size with several to a hundred atoms.[1−3] Particles in this size regime display discrete and size-tunable electronic transitions due to the strong quantum confinement of free electrons in the particles, thus leading to interesting molecule-like properties such as strong fluorescence.[4−12] Compared with common fluorophores such as organic dyes and semiconductor quantum dots (QDs), where practical deployment can be limited by relatively poor photostability (for organic fluorophores) or toxicity concerns (*e.g.*, QDs), fluorescent metal NCs are promising alternatives for the design of novel bioimaging probes because of their ultrafine size, excellent photostability, and low toxicity.[3,8,9] There is therefore strong interest in the development of synthesis methods for highly fluorescent metal NCs. This has led to the rapid expansion of reported procedures in the literature.

There are two main strategies for preparing fluorescent metal NCs. The first approach is the template-assisted synthesis. Here biomolecules (*e.g.*, proteins[5,13,14] and DNA[15−18]), dendrimers (*e.g.*, poly(amidoamine) (PAMAM)),[9,19] and polymers (*e.g.*, poly(methacrylic acid) (PMAA))[8,20−22] are used as a template to guide the formation of fluorescent Au and/or Ag NCs. However, the as-synthesized metal NCs are embedded in the template molecules, leading to a relatively large hydrodynamic diameter (>3 nm), which may affect their usability as a fluorescent label for small molecules or few-nanometer-sized biomolecules. The second approach relies on the use of specific capping agents, *e.g.*, thiol ligands, which interact strongly with the noble metal surface to form ultra-fine-sized metal NCs protected by a monolayer of thiol ligands.[23−32] Thiol-protected metal NCs have attractive features such as excellent stability, ultrasmall hydrodynamic diameters, and modifiable surface properties. Recent studies have shown that highly fluorescent Au and Ag NCs can be synthesized *via* the etching of

* E-mail: chexiej@nus.edu.sg. Tel: +65 6516 1067.

Received for review July 28, 2011 and accepted October 19, 2011.

Published online October 19, 2011
10.1021/nn202860s

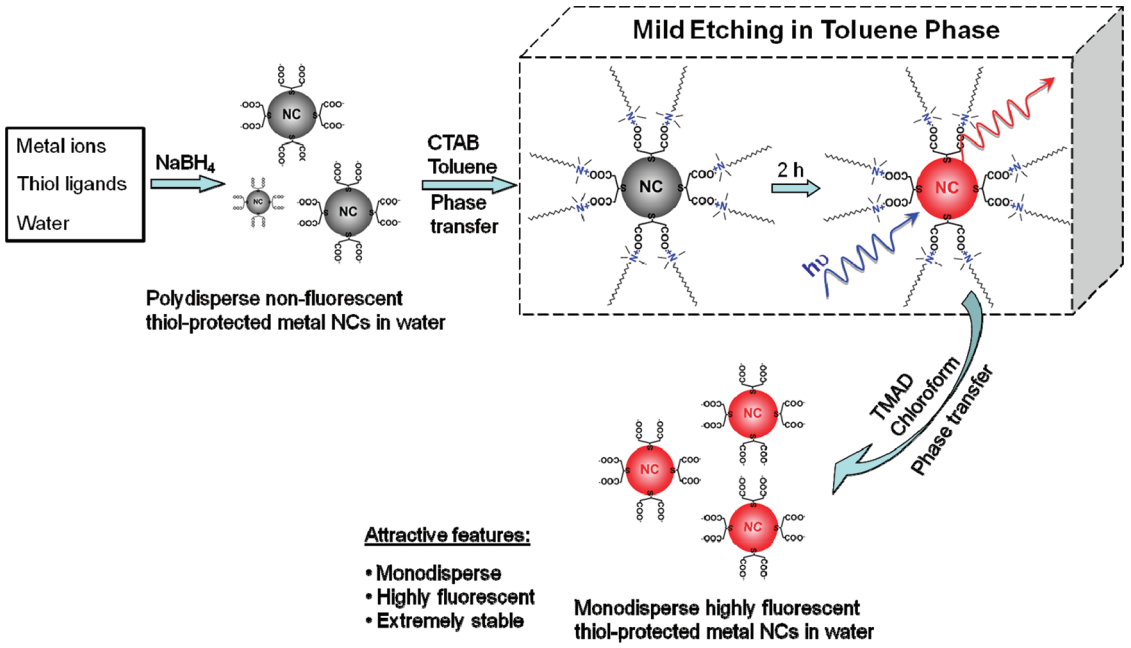

Scheme 1. Schematic illustration of the process to generate highly fluorescent metal NCs by a phase transfer cycle (aqueous → organic (incubation) → aqueous).

large metal nanoparticles (>3 nm) by excess ligands.[28,31,33−35] For example, Pradeep *et al.*[28] developed an interfacial etching method where mercaptosuccinic acid (MSA)-protected large Ag nanoparticles (>3 nm) in water were etched by excess MSA ligands in toluene to form fluorescent Ag NCs. The product formed after 48 h of interfacial etching was a mixture of large Ag nanoparticles and small blue- and red-emissive Ag NCs, where further processing (*e.g.*, electrophoresis) is needed to recover the fluorescent Ag NCs in sufficient purity. Furthermore, insofar as thiol-protected metal NCs are concerned, although there are a few reports on the synthesis of fluorescent Au NCs, the synthesis of Ag, Pt, and Cu analogues is even less attempted. To date, only fluorescent Ag_n (n = 7−9) NCs protected by MSA ligands have been successfully synthesized.[28,29] It would be of great interest to develop a facile and scalable method to fabricate thiol-protected fluorescent NCs of different metals, including Ag, Au, Pt, and Cu, to expand the repertoire of this potential new class of bioimaging probes, and to investigate composition/structure−property relationships.

Herein we report a simple and versatile synthesis of highly fluorescent Ag, Au, Pt, and Cu NCs based on a mild etching environment made possible by the electrostatically induced phase transfer of thiol-protected metal NCs from an aqueous solution to an organic phase. Using Ag as our model metal, a simple and fast (total synthesis time < 3 h) phase transfer cycle (aqueous → organic (2 h incubation) → aqueous) can process originally polydisperse, nonfluorescent, and unstable Ag NCs into monodisperse, highly fluorescent, and extremely stable Ag NCs in the same phase (aqueous) and protected by the same thiol ligand. Moreover, fluorescent Ag NCs with different functional groups on their surface (*e.g.*, carboxyl, hydroxyl, and amine) can be prepared by this phase transfer method using simple custom-designed peptide ligands with the desired functionalities. Presented below are the details of this investigation.

RESULTS AND DISCUSSION

The process for producing highly fluorescent metal NCs is simple and involves two steps. As shown in Scheme 1 (with more details in the Experimental Section), the first step is the synthesis of thiol-protected metal NCs by the reductive decomposition of thiolate-metal intermediates (using sodium borohydride, $NaBH_4$, as the reducing agent).[2] Glutathione (GSH), a common water-soluble thiol ligand, was selected as a model ligand. No fluorescence was detected for the as-prepared GSH-protected metal (Ag, Au, Pt, and Cu) NCs (insets of Figure 1, top item 2) in aqueous solution under UV illumination (365 nm).

The second step is the transfer of the GSH-protected metal NCs to an organic phase (toluene or hexane) *via* the electrostatic interaction ($(CTA)^+(COO)^-$) between negatively charged carboxyl groups (GSH has two carboxyl groups) on the metal NC surface and the positively charged cation of a hydrophobic salt, cetyltrimethylammonium bromide (CTAB) (Scheme 1).[36] This phase transfer occurs quickly upon mixing of the reagents. In our experiments a complete transfer of metal NCs from the aqueous phase to toluene was accomplished within 5 min. After incubation in toluene at room temperature for a fixed period of time

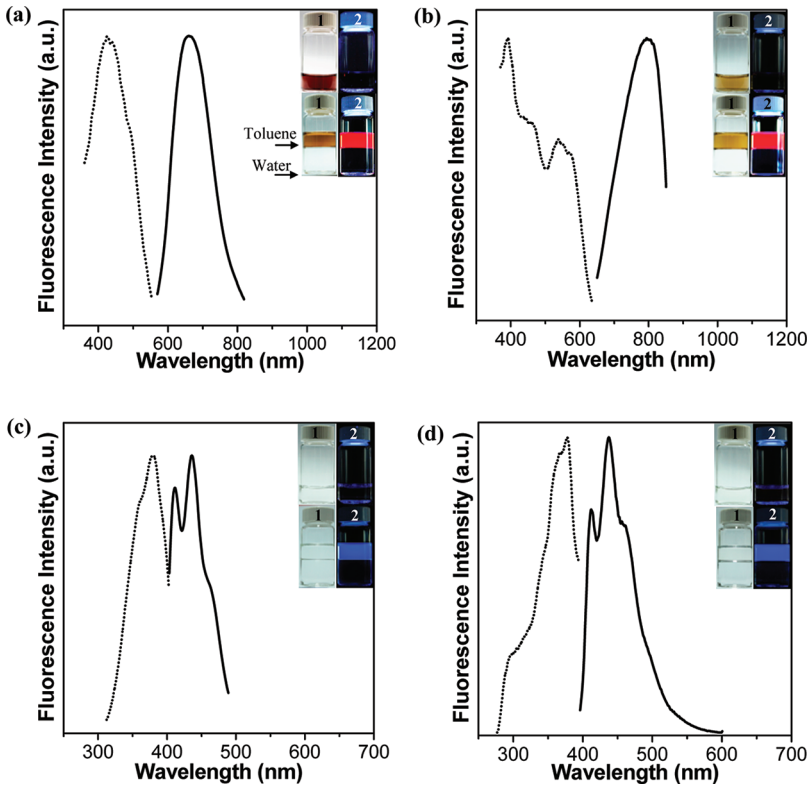

Figure 1. Photoexcitation (dotted lines) and photoemission (solid lines) spectra of the fluorescent Ag (a), Au (b), Pt (c), and Cu (d) NCs in toluene. The excitation spectra were measured at λ_{em} = 660, 700, 435, and 438 nm for (a) to (d), respectively, and the emission spectra were measured at λ_{ex}= 480, 540, 380, and 378 nm for (a) to (d), respectively. The insets show the digital photographs of the original metal NCs in water (top items 1 and 2) and the metal NCs in toluene (bottom items 1 and 2). Items 1 were viewed under visible light, whereas items 2 were viewed under UV light (365 nm).

(2 h for Ag and 24 h for Au, Pt, and Cu), strong fluorescence was observed in the toluene phase (insets of Figure 1, bottom item 2). Ag and Au NCs in toluene emitted an intense red fluorescence, while Pt and Cu NCs showed strong blue fluorescence. In comparison with the common ligand-exchange-induced phase transfer methods where the original hydrophilic capping ligands on the nanoparticle surface are displaced by hydrophobic ligands (or *vice versa*) with stronger binding affinity[37] and for which disadvantages such as the need for excess replacement ligands, slow and incomplete ligand exchange, limited ligand choices, and possible changes in the nanoparticle structure (due to the strong interaction between the replacement ligands and the metal nanoparticle surface) are known,[37,38] phase transfer *via* electrostatic interactions is fast and versatile and can be carried out under mild conditions without changing the capping ligands.

Control experiments using only GSH, CTAB, $NaBH_4$, and their mixtures without the addition of metal ions did not show any fluorescence, suggesting that the strong fluorescence in toluene was due to the ultrafine-sized metal NCs. The emission peak of the as-synthesized fluorescent Ag, Au, Pt, and Cu NCs in toluene was located at 660, 798, 410/436, and 412/438 nm, respectively (Figure 1). The quantum yield (QY) was 6.5%, 5.4%, 4.6%, and 3.5% for fluorescent Ag, Au, Pt, and Cu NCs, respectively (calibrated with rhodamine B for Ag and Au NCs and with quinoline for Pt and Cu NCs). Transmission electron microscopy (TEM) images (Figure S1 in Supporting Information) showed that the fluorescent metal (Ag, Au, Pt, and Cu) NCs in toluene were all below 2 nm in size. To the best of our knowledge, this is perhaps the first successful attempt in developing a simple method that can synthesize fluorescent NCs of four common metals (Ag, Au, Pt, and Cu). The synthetic protocol should also be applicable to bimetallic (*e.g.*, AgAu and AgPt) fluorescent NCs. In addition, the simplicity of phase transfer operations (*via* electrostatic interactions) also translates to process scalability. Volume production of fluorescent metal NCs can be easily realized by this method (Figure S2 in Supporting Information). Moreover, the as-synthesized fluorescent Ag, Au, Pt, and Cu NCs are protected by the same original ligand (GSH in this case) and can be used as a platform to develop fundamental composition−property relationships.

An added advantage of the current method is that the fluorescent metal NCs in the organic phase can be easily shuttled back to the aqueous phase. For example, upon the addition of a hydrophobic salt in chloroform, tetramethylammonium decanoate (TMAD), to the fluorescent metal NCs in toluene, the hydrophobic decanoate anion D^- quickly formed a hydrophobic salt

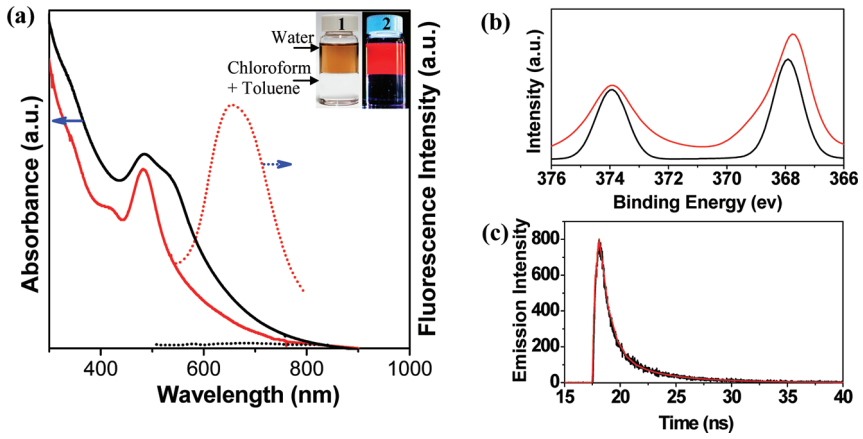

Figure 2. (a) Optical absorption (solid lines) and photoemission (dotted lines) spectra of the orginal GSH-protected Ag NCs (black lines) and the returned fluorescent GSH-protected Ag NCs (red lines) in the aqueous phase. The inset shows photographs of the returned fluorescent GSH-protected Ag NCs in the aqueous phase under visible (item 1) and UV (item 2) light. (b) XPS spectrum of the returned fluorescent GSH-protected Ag NCs (red line) and GSH−Ag^{I} complex intermediates (black line). (c) Time-resolved fluorescence lifetime analysis of the returned fluorescent GSH-protected Ag NCs (black line). The red line is a biexponential fit of the experimental data.

$(CTA)^{+}D^{-}$ with the hydrophobic cation CTA^{+} on the GSH-protected metal NCs. The removal of the hydrophobic cation CTA^{+} from the GSH-protected metal NCs restored the negative charge (from the carboxyl groups of GSH) on the metal NCs, enabling them to return back to the aqueous phase. Fast (<5 min) and complete (>90 mol %) transfer of the fluorescent metal NCs from the organic (mixture of chloroform and toluene) to the aqueous phase was made possible by this method. It should be mentioned that there were no CTA^{+} ions associated with the fluorescent metal NCs returned back to the aqueous phase (see Figure S3 in Supporting Information for the Fourier transform infrared spectroscopy (FTIR) analysis of fluorescent GSH-protected Ag NCs in aqueous solution). The phase transfer reversibility of fluorescent metal NCs between organic and aqueous solutions broadened the usability of these NCs in both organic and aqueous environments.

Using Ag as an example, we demonstrated that a phase transfer cycle (aqueous → organic (incubation) → aqueous) could efficiently process the original nonfluorescent GSH-protected Ag NCs (inset of Figure 1a, top item) in aqueous phase to highly fluorescent Ag NCs (inset of Figure 2a) also in the aqueous phase. As shown in Figure 2a, the Ag NCs after one phase transfer cycle showed a strong emission peak at 660 nm (dotted red line), whereas the original Ag NCs did not display any emission in the same wavelength regime (dotted black line). It is known experimentally and theoretically that ultra-fine-sized (<2 nm) metal NCs acquire molecule-like absorption features, which are related to their size-dependent discrete energy levels.[1,4,9,39,40] The fluorescent Ag NCs returned to the aqueous phase exhibited a well-defined optical absorption spectrum with a prominent sharp peak at 480 nm and a very narrow full width at half-maximum (fwhm) of <45 nm (Figure 2a, solid red line), characteristic of highly monodisperse Ag NCs. On the contrary, the original Ag NCs in aqueous solution showed broad absorption peaks at 480 and 540 nm (Figure 2a, solid black line), reflecting the polydisperse nature of the original Ag NCs. TEM images also confirmed that the returned fluorescent Ag NCs (Figure S4a in Supporting Information) were more monodisperse than the original Ag NCs (Figure S4b in Supporting Information). The STEM image (inset of Figure S4a in Supporting Information) measured the size of the returned fluorescent Ag NC as approximately 1.5 nm. Recently, Kumar *et al.* reported a family of discrete-sized Ag NCs protected by GSH *via* the electrophoretic separation of a Ag NC mixture.[41] The absorption spectrum of our fluorescent Ag NCs was similar to that of the GSH-protected Ag_{29} NCs in that study (most notably the characteristic narrow absorption peak at 480 nm).[41] Since the same protecting ligand (GSH) was used in both studies, it is reasonable to consider our fluorescent Ag NCs as Ag_{29} NCs. Furthermnore, elemental analyses of the fluorescent Ag NCs by thermal gravimetric analysis (TGA) (Figure S5 in Supporting Information) and energy-dispersive X-ray spectroscopy (EDX) (Figure S6 in Supporting Information) showed a Ag to GSH molar ratio of approximately 1.30 and 1.34, respectively, which are quite close to the molar ratio estimated for $Ag_{29}(GSH)_{22}$ (~1.32). However, more detailed information on the exact composition and the cluster structure of the as-synthesized Ag NCs has to await systematic studies based on mass spectrometry (*e.g.*, MALDI-TOF and ESI-MS) and total crystal structure determination.

The oxidation state of fluorescent Ag NCs was examined by X-ray photoelectron spectroscopy (XPS). The binding energy of Ag $3d_{5/2}$ of fluorescent Ag NCs (Figure 2b, red line) was 367.7 eV. In contrast, the Ag $3d_{5/2}$ binding energy of thiolate−Ag^{I} complex

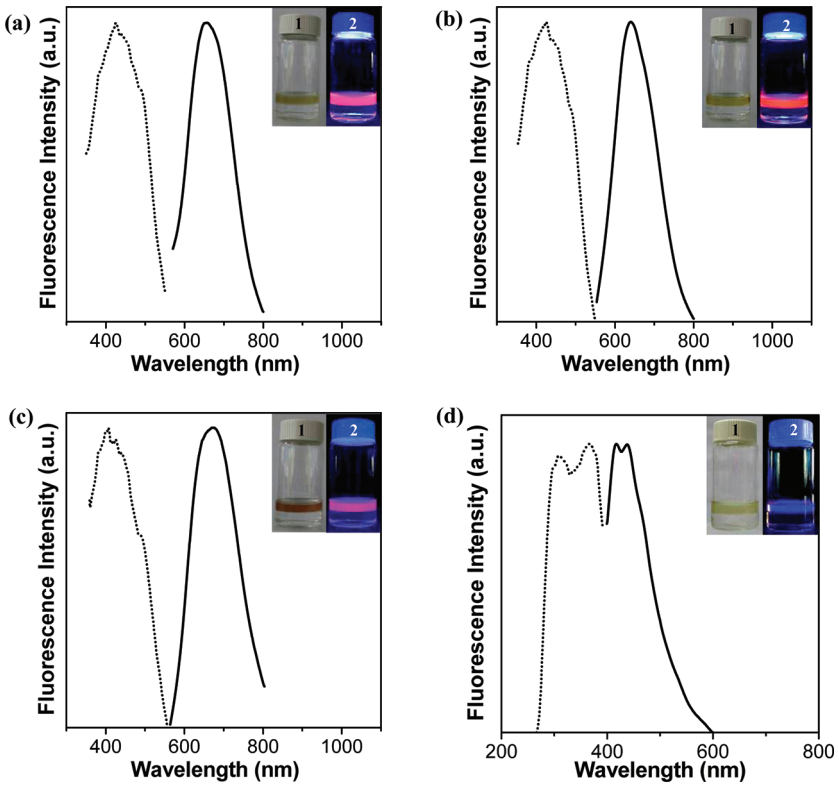

Figure 3. Photoexcitation (dotted lines) and photoemission (solid lines) spectra of fluorescent Ag NCs synthesized by Glu-Cys-Glu (a), Asp-Cys-Asp (b), Ser-Cys-Ser (c), and Lys-Cys-Lys (d). The excitation spectra were measured at λ_{em} = 655, 640, 670, and 440 nm for (a) to (d), respectively, and the emission spectra were measured at λ_{ex} = 480 nm for (a) to (c) and 368 nm for (d). The insets are photographs of Ag NCs synthesized by the different peptides under visible (item 1) and UV (item 2) light.

intermediates (simply prepared by the mixing of GSH with $AgNO_3$ solution) was 367.9 eV (Figure 2b, black line). A slight shift of 0.2 eV of Ag $3d_{5/2}$ binding energy indicates that the Ag NCs had an oxidation state different from that of the thiolate–Ag^I complex intermediates. Analysis of the luminescence decay of the fluorescent Ag NCs at 660 nm revealed a decay response on the nanosecond scale that can be fitted to a biexponential function (Figure 2c, red line) with fast (0.96 ns, 81%) and slow (4.4 ns, 19%) components in different ratios. The short lifetimes of our fluorescent Ag NCs are similar to the nanosecond emission from the singlet excited states of water-soluble Ag^0 NCs protected by polymers[21] or DNA.[42]

Versatility is another suit of the electrostatically induced phase transfer method since the thiol ligands can be designed to introduce additional functionalities to the fluorescent metal NC surface to increase the usability of the latter in biolabeling and bioimaging applications. For example thiol ligands can be designed as peptides to impart biocompatibility and limitless diversity and to reduce the environmental footprint of the synthesis.[43,44] The glutathione (GSH) used in this study is indeed a tripeptide with glutamic acid, cysteine, and glycine residues. The thiol group from the cysteine residue is essential for the formation of ultra-fine-sized metal NCs (<2 nm) in this study, without which (*e.g.*, when GSH was replaced by a glutamic acid-serine-glycine peptide) only large and nonfluorescent nanoparticles (>2 nm) were formed (Figure S7 in Supporting Information). Hence the designed peptides must contain at least one thiol group (*e.g.*, from cysteine) together with amino acids with other functional side groups (*e.g.*, carboxyl, hydroxyl, and amine) to introduce the desired functionalities to the metal NC surface. As a proof of concept, we have designed several simple tripeptides, X–cysteine–X (X indicates any natural amino acid), for the synthesis of fluorescent Ag NCs. Three types of residues were used for X: (a) X = aspartic and glutamic acid to represent negatively charged carboxyl side groups; (b) X = serine to represent neutral hydroxyl side groups; and (c) X = lysine to represent positively charged amine side groups. As shown in Figure 3, intense red-emissive Ag NCs were synthesized by Asp-Cys-Asp, Glu-Cys-Glu, and Ser-Cys-Ser peptides, while strong blue-emissive Ag NCs were synthesized by Lys-Cys-Lys. Given that there are innumerous peptides that can be designed with the thiol group, fluorescent metal NCs with the desired functionalities can be prepared through simple customizations (*e.g.*, changing the number of cysteine residues, length, functionalities, and structure) of the peptide ligands and using the reversible phase transfer method of this study to create NC fluorescence.

While it is not clear at the molecular level how the phase transfer of Ag NCs from aqueous to organic

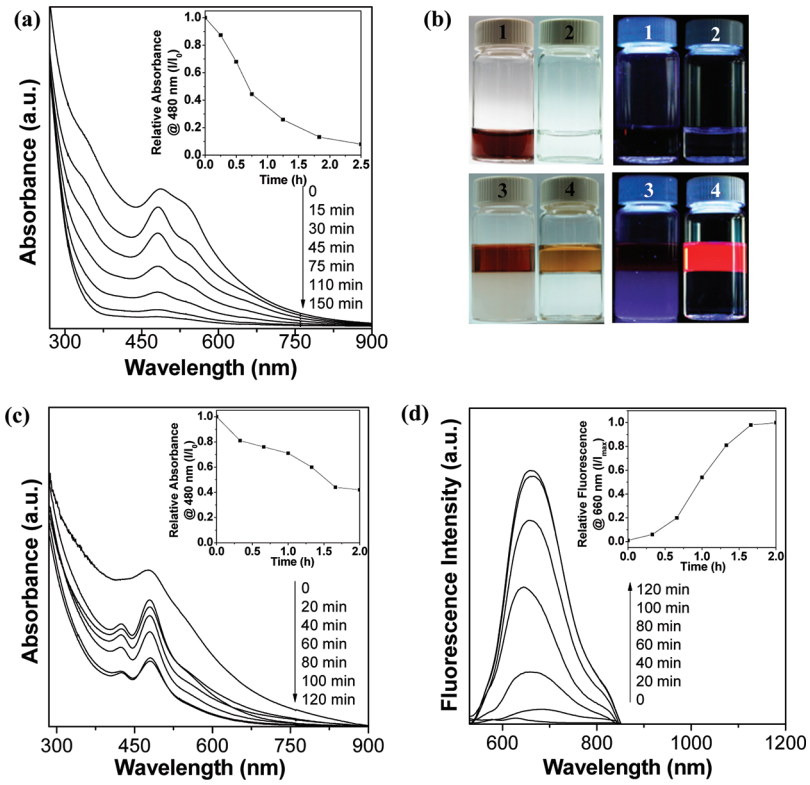

Figure 4. (a) Time-resolved evolution of optical absorption spectra of the original Ag NCs in water, indicating complete decomposition of the NCs within 2.5 h. The inset shows relative optical absorption intensity ($I/I_{original}$) at 480 nm as a function of time. (b) Photographs of the original Ag NCs in water immediately after preparation (item 1) and after incubation for 2.5 h at room temperature (item 2); Ag NCs tranfered to toluene immediately after preparation (item 3) and after incubation in toluene for 2 h at room temperature (item 4). The left panel shows the solution in visible light, and the right panel is viewed under UV illumination. Time-resolved evolution of optical absorption (c) and photoemission (d) spectra of Ag NCs in toluene. The inset in (c) shows relative optical absorption intensity (I/I_0) at 480 nm, and the inset in (d) shows relative fluorescence intensity ($I/I_{2\ h}$), as a function of time.

phase followed by a short incubation in the latter generated fluorescence of Ag NCs, there were two revealing observations: (i) The concentration ratio of GSH to Ag precursor ($R_{[GSH]/[Ag]}$) was critical. At a fixed Ag precursor concentration (0.5 mM), a relatively high concentration ratio ($R_{[GSH]/[Ag]} \geq 3$) was required for the synthesis of highly fluorescent Ag NCs (Figures S8 and S9 in Supporting Information). Decreasing the ratio to 1 and below would only produce nonfluorescent, large Ag nanoparticles (>2 nm) with characteristic surface plasmon resonance (SPR) at approximately 405 nm (Figure S8a in Supporting Information).

(ii) The etching of Ag NCs in toluene was much slower than in the aqueous phase. The mild etching environment made possible by phase transfer *via* electrostatic interactions seems to favor the formation of stable Ag NCs with a well-defined structure (other metastable NC species were gradually decomposed by this "size-focusing" process).[7] The strong fluorescence observed in the organic phase was most likely emitted by these stable Ag NCs with a well-defined structure.

Control experiments showed that the original GSH-protected Ag NCs degraded rather rapidly in the aqueous phase, as shown by the diminishing absorption peaks in their UV–vis spectra (Figure 4a) as well as solution color change. The original deep-red Ag NCs in the aqueous solution (Figure 4b, left panel, item 1) was etched to colorless (item 2) in 2.5 h. This was due to the decomposition of the original Ag NCs to thiolate–Ag^I complex and confirmed by the time-course measurements of changes in the absorption spectra (Figure 4a). The facile decomposition of original Ag NCs in the aqueous solution was not unexpected, considering that thiol ligands are strong etchants for small Ag NCs and the ease of oxidation of atomic Ag in the presence of oxygen (from air).[7,28,45] No fluorescence was emitted by the original Ag NCs or the decomposed Ag NCs (thiolate–Ag^I complex) in aqueous solution (Figure 4b, items 1 and 2, right panel).

On the contrary, Ag NCs after phase transfer to an organic phase decomposed much more slowly, possibly because most of the free hydrophilic thiol ligands ("etchants") were left behind in the aqueous solution. Since the bromide anion from the phase transfer agent CTAB is a potential etchant for the ultrasmall Ag NCs, a control experiment was carried out where a bromide-free phase transfer agent (dodecylamine (DDA)) was used. Ag NCs with a red fluorescence were still formed (Figure S10 in Supporting Information), thereby ruling

out bromide as a possible cause for the formation of fluorescent Ag NCs in the current study.

More gradual changes in the absorption spectra and solution color provided the direct evidence for the slower decomposition in the organic phase. As shown in Figure 4b (left panel), the as-transferred Ag NCs in toluene were intense red in color (item 3) and faded to a lighter color slowly in toluene (item 4, a typical sample after 2 h incubation). In addition, the absorption peak of Ag NCs in toluene at 480 nm became much sharper (Figure 4c, 20 min), indicating the size-focusing of Ag NCs in toluene due to the etching of metastable Ag NC species.[7] Accordingly, fluorescent Ag NC species were gradually formed. The evolution of the emission spectra of Ag NCs in toluene is shown in Figure 4d. While the initial Ag NCs in toluene exhibited no visible emission, an intense emission band centering at 660 nm appeared 20 min later upon excitation at 480 nm. The fluorescence intensity increased gradually with the increase in incubation time. Maximum emission intensity occurred at an incubation time of approximately 2 h. Further incubation was found to slowly decrease the fluorescence intensity. However, it is noteworthy to mention that the fluorescence could still be observed after incubation for up to 3 days at room temperature. Improved stability of the as-synthesized fluorescent Ag NCs in the organic phase was possible if they were stored at a low temperature (*e.g.*, 4 °C) and in an inert gas atmosphere (*e.g.*, N_2). In that case, the fluorescence intensity loss was less than 20% after 6 months of storage.

Further stability improvement of the fluorescent Ag NCs was achieved by transferring the Ag NCs back to the aqueous phase. Since the fluorescence intensity in the organic phase was maximum after 2 h of incubation, 2 h was selected as the optimal incubation time. The fluorescent Ag NCs after 2 h of incubation and returning to the aqueous phase exhibited more persistent fluorescence; the fluorescence loss was <10% even after 6 months' storage at 4 °C and without the protection of a N_2 blanket (Figure S11 in Supporting Information). The good stability of the final fluorescent Ag NCs in aqueous solution could be attributed to the formation of extraordinarily stable Ag NC species with a well-defined structure, in addition to the purification of products from free ligands and byproduct by phase transfer operations. The improved stability of the final products can greatly improve their usability in biomedical and other sensing applications.

CONCLUSION

In summary, we have developed a new method for generating highly fluorescent Ag, Au, Pt, and Cu NCs in a mild etching environment made possible by phase transfer *via* electrostatic interactions. Using Ag as a model metal, we demonstrated a simple and fast (total synthesis time < 3 h) phase transfer cycle (aqueous → organic (2 h incubation) → aqueous) whereby polydisperse, nonfluorescent, and unstable Ag NCs in aqueous solution could be transformed into monodisperse, highly fluorescent, and extremely stable Ag NCs in aqueous solution protected by the same original thiol ligand (GSH). The synthetic protocol was then extended to fabricate highly fluorescent Ag NCs protected by custom-designed peptides with different functionalities (*e.g.*, carboxyl, hydroxyl, and amine). The attractive features of these metal (Ag, Au, Pt, and Cu) NCs, such as an ultrasmall hydrodynamic diameter, high stability, biocompatible protecting ligands, and excellent fluorescence properties, are likely to promote their acceptance in bioimaging and biosensing applications.

EXPERIMENTAL SECTION

Materials and Instruments. Silver nitrate ($AgNO_3$), sodium hydroxide, ethanol, and methanol from Merck; hexachloroplatinic acid hexahydrate (H_2PtCl_6), copper sulfate pentahydrate ($CuSO_4$), L-glutathione reduced (GSH), sodium borohydride ($NaBH_4$), cetyltrimethylammonium bromide (CTAB), decanoic acid (DA), dodecylamine (DDA), and tetramethylammonium hydroxide pentahydrate (TMAH) from Sigma-Aldrich; peptides Glu-Cys-Glu (ECE), Asp-Cys-Asp (DCD), Ser-Cys-Ser (SCS), Lys-Cys-Lys (KCK), and Glu-Ser-Gly (ESG) from GL Biochem (Shanghai) Ltd.; hydrogen tetrachloroaurate(III) trihydrate ($HAuCl_4$) from Alfa Aesar; toluene from Tedia; and chloroform from Fisher were used as received. Ultrapure Millipore water (18.2 MΩ) was used. All glassware was washed with *aqua regia* and rinsed with ethanol and ultrapure water.

UV−vis and fluorescence spectra were recorded on a Shimadzu UV-1800 spectrometer and a PerkinElmer LS55 fluorescence spectrometer, respectively. Transmission electron microscopy images were taken on a JEOL JEM 2010 microscope operating at 200 kV. Scanning electron microscopy and energy dispersive X-ray spectroscopy were performed on a field emission scanning electron microscope (JEOL JSM-7400F) operating at 25.0 kV. Fluorescence lifetime was counted on a Picoquant FluoTime 300 automated fluorescence lifetime spectrometer. X-ray photoelectron spectroscopy was performed on a VG ESCALAB MKII spectrometer. The efficiency of phase transfer was analyzed by inductively coupled plasma mass spectroscopy (ICP-MS) on an Agilent 7500A. Thermogravimetric analysis was measured on a Shimadzu TGA-60 analyzer under a N_2 atmosphere (flow rate of 100 mL·min^{-1}). Fourier transform infrared spectra were obtained on a Shimadzu IR Prestige-21 FTIR spectrophotometer.

Synthesis of the Original Metal NCs in the Aqueous Phase. Aqueous stock solutions of metal precursors ($AgNO_3$, $HAuCl_4$, H_2PtCl_6, and $CuSO_4$) with concentrations of 20 mM and aqueous solutions of thiol ligands (GSH and peptides (ECE, DCD, SCS, and KCK)) with concentrations of 50 mM were prepared with ultrapure water. An aqueous $NaBH_4$ solution with a concentration of 112 mM was freshly prepared by dissolving 43 mg of $NaBH_4$ in 8 mL of ultrapure water, followed by the addition of 2 mL of 1 M NaOH solution. The addition of a small amount of NaOH to $NaBH_4$ solution helped to improve the stability of borohydride ions against hydrolysis.[46] In a typical experiment to synthesize

the original metal NCs in the aqueous phase, GSH solution (150 μL, 50 mM), $NaBH_4$ solution (50 μL, 112 mM), and metal precursor solution (125 μL, 20 mM) were added sequentially to water (4.85 mL) under vigorous stirring. The original metal NCs in aqueous solution were collected after 10 min. The syntheses of the original Ag NCs protected by other peptide ligands (ECE, DCD, SCS, and KCK) were carried out under similar conditions except for the replacement of GSH by the other peptide ligands.

Phase Transfer from Aqueous to Toluene. CTAB in ethanol (5 mL, 100 mM) was introduced to the original metal NCs in aqueous solution (~5 mL), and the mixture was stirred for 20 s. Toluene (5 mL) and aqueous NaOH (15 μL, 1 M) were then added sequentially, and stirring continued for one more minute. The addition of a small amount of NaOH is to enhance the interaction between cation CTA^+ and anion carboxyl (COO^-, from GSH), thus facilitating the phase transfer process. Metal NCs were completely transferred to the toluene phase within 5 min. Without stirring, the as-transferred metal NCs in toluene were incubated at room temperature for a certain period of time (2 h for Ag and 24 h for Au, Pt, and Cu). Strong fluorescent metal NCs can then be observed in the toluene phase.

Phase Transfer from Organic to Aqueous. Hydrophobic tetramethylammonium decanoate was used to transfer the fluorescent Ag NCs back to the aqueous phase. Stock methanolic TMAD solution was prepared by dissolving DA (1.7 g) and TMAH (1.8 g) to 100 mL of methanol. In a typical phase transfer experiment, the fluorescent Ag NCs in toluene (5 mL) were collected, followed by the sequential addition of chloroform (5 mL), water (5 mL), and TMAD (5 mL). The mixture was stirred for 1 min. The fluorescent Ag NCs were then transferred back to the aqueous phase.

Acknowledgment. This work is financially supported by the Ministry of Education, Singapore, under Grants R-279-000-295-133 and R-279-000-327-112.

Supporting Information Available: Figure S1, TEM images of the fluorescent Ag, Au, Pt, and Cu NCs in toluene; Figure S2, photographs of fluorescent Ag NCs synthesized in a 500 mL bottle; Figure S3–S6, FTIR, TEM (STEM), TGA, and EDX analysis of the as-synthesized fluorescent Ag NCs; Figure S7, optical absorption spectrum and TEM image of Ag nanoparticles synthesized by a tripeptide without cysteine (Glu-Ser-Gly); Figure S8, optical absorption spectra, photographs, and TEM images of the original Ag NCs formed under different concentration ratios ($R_{[GSH]/[Ag]}$); Figure S9, photoemission spectra and photographs of the as-synthesized Ag NCs in tolune under different concentration ratios ($R_{[GSH]/[Ag]}$); Figure S10, optical absorption, photoemission, and photopraphs of the fluorescent Ag NCs synthesized by DDA; Figure S11, photoemission spectra of the final fluorescent Ag NCs in the aqueous phase freshly prepared and after 6 months' storage. This material is available free of charge *via* the Internet at http://pubs.acs.org.

REFERENCES AND NOTES

1. Jin, R. C. Quantum Sized, Thiolate-Protected Gold Nanoclusters. *Nanoscale* **2010**, *2*, 343–362.
2. Zhang, Q. B.; Xie, J. P.; Yu, Y.; Lee, J. Y. Monodispersity Control in the Synthesis of Monometallic and Bimetallic Quasi-Spherical Gold and Silver Nanoparticles. *Nanoscale* **2010**, *2*, 1962–1975.
3. Diez, I.; Ras, R. H. A. Fluorescent Silver Nanoclusters. *Nanoscale* **2011**, *3*, 1963–1970.
4. Laaksonen, T.; Ruiz, V.; Liljeroth, P.; Quinn, B. M. Quantised Charging of Monolayer-Protected Nanoparticles. *Chem. Soc. Rev.* **2008**, *37*, 1836–1846.
5. Xie, J. P.; Zheng, Y. G.; Ying, J. Y. Protein-Directed Synthesis of Highly Fluorescent Gold Nanoclusters. *J. Am. Chem. Soc.* **2009**, *131*, 888–889.
6. Santiago González, B.; Rodríguez, M. a. J.; Blanco, C.; Rivas, J.; López-Quintela, M. A.; Martinho, J. M. G. One Step Synthesis of the Smallest Photoluminescent and Paramagnetic PVP-Protected Gold Atomic Clusters. *Nano Lett.* **2010**, *10*, 4217–4221.
7. Jin, R.; Qian, H.; Wu, Z.; Zhu, Y.; Zhu, M.; Mohanty, A.; Garg, N. Size Focusing: A Methodology for Synthesizing Atomically Precise Gold Nanoclusters. *J. Phys. Chem. Lett.* **2010**, *1*, 2903–2910.
8. Xu, H.; Suslick, K. S. Water-Soluble Fluorescent Silver Nanoclusters. *Adv. Mater.* **2010**, *22*, 1078–1082.
9. Zheng, J.; Nicovich, P. R.; Dickson, R. M. Highly Fluorescent Noble-Metal Quantum Dots. *Annu. Rev. Phys. Chem.* **2007**, *58*, 409–431.
10. Peyser, L. A.; Vinson, A. E.; Bartko, A. P.; Dickson, R. M. Photoactivated Fluorescence from Individual Silver Nanoclusters. *Science* **2001**, *291*, 103–106.
11. Tanaka, S.-I.; Miyazaki, J.; Tiwari, D. K.; Jin, T.; Inouye, Y. Fluorescent Platinum Nanoclusters: Synthesis, Purification, Characterization, and Application to Bioimaging. *Angew. Chem., Int. Ed.* **2011**, *50*, 431–435.
12. Wei, W.; Lu, Y.; Chen, W.; Chen, S. One-Pot Synthesis, Photoluminescence, and Electrocatalytic Properties of Subnanometer-Sized Copper Clusters. *J. Am. Chem. Soc.* **2011**, *133*, 2060–2063.
13. Liu, C.-L.; Wu, H.-T.; Hsiao, Y.-H.; Lai, C.-W.; Shih, C.-W.; Peng, Y.-K.; Tang, K.-C.; Chang, H.-W.; Chien, Y.-C.; Hsiao, J.-K.; *et al.* Insulin-Directed Synthesis of Fluorescent Gold Nanoclusters: Preservation of Insulin Bioactivity and Versatility in Cell Imaging. *Angew. Chem., Int. Ed.* **2011**, *50*, 7056–7060.
14. Xie, J. P.; Zheng, Y. G.; Ying, J. Y. Highly Selective and Ultrasensitive Detection of Hg^{2+} Based on Fluorescence Quenching of Au Nanoclusters by Hg^{2+}-Au^+ Interactions. *Chem. Commun.* **2010**, *46*, 961–963.
15. Petty, J. T.; Zheng, J.; Hud, N. V.; Dickson, R. M. DNA-Templated Ag Nanocluster Formation. *J. Am. Chem. Soc.* **2004**, *126*, 5207–5212.
16. Koszinowski, K.; Ballweg, K. A Highly Charged Ag_{64}^+ Core in a DNA-Encapsulated Silver Nanocluster. *Chem.—Eur. J.* **2010**, *16*, 3285–3290.
17. Richards, C. I.; Choi, S.; Hsiang, J.-C.; Antoku, Y.; Vosch, T.; Bongiorno, A.; Tzeng, Y.-L.; Dickson, R. M. Oligonucleotide-Stabilized Ag Nanocluster Fluorophores. *J. Am. Chem. Soc.* **2008**, *130*, 5038–5039.
18. Gwinn, E. G.; O'Neill, P.; Guerrero, A. J.; Bouwmeester, D.; Fygenson, D. K. Sequence-Dependent Fluorescence of DNA-Hosted Silver Nanoclusters. *Adv. Mater.* **2008**, *20*, 279–283.
19. Zheng, J.; Zhang, C. W.; Dickson, R. M. Highly Fluorescent, Water-Soluble, Size-Tunable Gold Quantum Dots. *Phys. Rev. Lett.* **2004**, *93*, 077402-1–077402-4.
20. Xu, H. X.; Suslick, K. S. Sonochemical Synthesis of Highly Fluorescent Ag Nanoclusters. *ACS Nano* **2010**, *4*, 3209–3214.
21. Shang, L.; Dong, S. J. Facile Preparation of Water-Soluble Fluorescent Silver Nanoclusters Using a Polyelectrolyte Template. *Chem. Commun.* **2008**, *9*, 1088–1090.
22. Shen, Z.; Duan, H.; Frey, H. Water-Soluble Fluorescent Ag Nanoclusters Obtained from Multiarm Star Poly(acrylic acid) as "Molecular Hydrogel" Templates. *Adv. Mater.* **2007**, *19*, 349–352.
23. Zhu, M.; Aikens, C. M.; Hollander, F. J.; Schatz, G. C.; Jin, R. Correlating the Crystal Structure of a Thiol-Protected Au_{25} Cluster and Optical Properties. *J. Am. Chem. Soc.* **2008**, *130*, 5883–5885.
24. Wu, Z. K.; Jin, R. C. On the Ligand's Role in the Fluorescence of Gold Nanoclusters. *Nano Lett.* **2010**, *10*, 2568–2573.
25. Wu, Z.; Lanni, E.; Chen, W.; Bier, M. E.; Ly, D.; Jin, R. High Yield, Large Scale Synthesis of Thiolate-Protected Ag_7 Clusters. *J. Am. Chem. Soc.* **2009**, *131*, 16672–16674.
26. Qian, H. F.; Zhu, Y.; Jin, R. C. Size-Focusing Synthesis, Optical and Electrochemical Properties of Monodisperse $Au_{38}(SC_2H_4Ph)_{24}$ Nanoclusters. *ACS Nano* **2009**, *3*, 3795–3803.
27. Bakr, O. M.; Amendola, V.; Aikens, C. M.; Wenseleers, W.; Li, R.; Dal Negro, L.; Schatz, G. C.; Stellacci, F. Silver Nanoparticles with Broad Multiband Linear Optical Absorption. *Angew. Chem., Int. Ed.* **2009**, *48*, 5921–5926.
28. Udaya Bhaskara Rao, T.; Pradeep, T. Luminescent Ag_7 and Ag_8 Clusters by Interfacial Synthesis. *Angew. Chem., Int. Ed.* **2010**, *49*, 3925–3929.

29. Rao, T. U. B.; Nataraju, B.; Pradeep, T. Ag_9 Quantum Cluster Through a Solid-State Route. *J. Am. Chem. Soc.* **2010**, *132*, 16304–16307.
30. Diez, I.; Jiang, H.; Ras, R. H. A. Enhanced Emission of Silver Nanoclusters Through Quantitative Phase Transfer. *Chem. Phys. Chem.* **2010**, *11*, 3100–3104.
31. Muhammed, M. A. H.; Verma, P. K.; Pal, S. K.; Kumar, R. C. A.; Paul, S.; Omkumar, R. V.; Pradeep, T. Bright, NIR-Emitting Au_{23} from Au_{25}: Characterization and Applications Including Biolabeling. *Chem.—Eur. J.* **2009**, *15*, 10110–10120.
32. Cathcart, N.; Kitaev, V. Silver Nanoclusters: Single-Stage Scaleable Synthesis of Monodisperse Species and Their Chirooptical Properties. *J. Phys. Chem. C* **2010**, *114*, 16010–16017.
33. Huang, C. C.; Yang, Z.; Lee, K. H.; Chang, H. T. Synthesis of Highly Fluorescent Gold Nanoparticles for Sensing Mercury(II). *Angew. Chem., Int. Ed.* **2007**, *46*, 6824–6828.
34. Zhou, R. J.; Shi, M. M.; Chen, X. Q.; Wang, M.; Chen, H. Z. Atomically Monodispersed and Fluorescent Sub-Nanometer Gold Clusters Created by Biomolecule-Assisted Etching of Nanometer-Sized Gold Particles and Rods. *Chem.—Eur. J.* **2009**, *15*, 4944–4951.
35. Lin, C. A. J.; Yang, T. Y.; Lee, C. H.; Huang, S. H.; Sperling, R. A.; Zanella, M.; Li, J. K.; Shen, J. L.; Wang, H. H.; Yeh, H. I.; *et al.* Synthesis, Characterization, and Bioconjugation of Fluorescent Gold Nanoclusters Toward Biological Labeling Applications. *ACS Nano* **2009**, *3*, 395–401.
36. Wei, Y. F.; Yang, J.; Ying, J. Y. Reversible Phase Transfer of Quantum Dots and Metal Nanoparticles. *Chem. Commun.* **2010**, *46*, 3179–3181.
37. Yang, J.; Lee, J. Y.; Ying, J. Y. Phase Transfer and Its Applications in Nanotechnology. *Chem. Soc. Rev.* **2011**, *40*, 1672–1696.
38. Knoppe, S.; Dharmaratne, A. C.; Schreiner, E.; Dass, A.; Bürgi, T. Ligand Exchange Reactions on Au_{38} and Au_{40} Clusters: A Combined Circular Dichroism and Mass Spectrometry Study. *J. Am. Chem. Soc.* **2010**, *132*, 16783–16789.
39. Akola, J.; Walter, M.; Whetten, R. L.; Hakkinen, H.; Gronbeck, H. On the Structure of Thiolate-Protected Au_{25}. *J. Am. Chem. Soc.* **2008**, *130*, 3756–3657.
40. Negishi, Y.; Takasugi, Y.; Sato, S.; Yao, H.; Kimura, K.; Tsukuda, T. Magic-Numbered Au_n Clusters Protected by Glutathione Monolayers (n = 18, 21, 25, 28, 32, 39): Isolation and Spectroscopic Characterization. *J. Am. Chem. Soc.* **2004**, *126*, 6518–6519.
41. Kumar, S.; Bolan, M. D.; Bigioni, T. P. Glutathione-Stabilized Magic-Number Silver Cluster Compounds. *J. Am. Chem. Soc.* **2010**, *132*, 13141–13143.
42. Vosch, T.; Antoku, Y.; Hsiang, J. C.; Richards, C. I.; Gonzalez, J. I.; Dickson, R. M. Strongly Emissive Individual DNA-Encapsulated Ag Nanoclusters As Single-Molecule Fluorophores. *Proc. Natl. Acad. Sci. U. S. A.* **2007**, *104*, 12616–12621.
43. Tan, Y. N.; Lee, J. Y.; Wang, D. I. C. Uncovering the Design Rules for Peptide Synthesis of Metal Nanoparticles. *J. Am. Chem. Soc.* **2010**, *132*, 5677–5686.
44. Xie, J. P.; Lee, J. Y.; Wang, D. I. C.; Ting, Y. P. Silver Nanoplates: From Biological to Biomimetic Synthesis. *ACS Nano* **2007**, *1*, 429–439.
45. Wiley, B.; Herricks, T.; Sun, Y.; Xia, Y. Polyol Synthesis of Silver Nanoparticles: Use of Chloride and Oxygen to Promote the Formation of Single-Crystal, Truncated Cubes and Tetrahedrons. *Nano Lett.* **2004**, *4*, 1733–1739.
46. Martin, M. N.; Basham, J. I.; Chando, P.; Eah, S. K. Charged Gold Nanoparticles in Non-Polar Solvents: 10-min Synthesis and 2D Self-Assembly. *Langmuir* **2010**, *26*, 7410–7417.